Aerodynamic stabilization of central stabilizers for box girder suspension bridges

Yaojun Ge, Xiaojie Zou and Yongxin Yang*

*State Key Laboratory for Disaster Reduction in Civil Engineering,
Tongji University, Shanghai 200092, China*

Abstract. For long-span suspension bridges with their intrinsic limit in flutter, some counter measures, for example, central stabilizers, should be adopted to improve aerodynamic stability to meet with the appropriate wind resistance requirements. The present paper introduces aerodynamic stabilization for long-span suspension bridges with box girders by using central stabilizers based on Xihoumen Bridge with the main span of 1650 m. The aerodynamic stabilization study covers experimental investigation of sectional model testing, comprehensive evaluation of three central stabilizers and theoretical analysis of stabilizing mechanism related to flutter derivatives, aerodynamic damping and degree participation.

Keywords: suspension bridge; flutter stabilization; flutter mechanism; box girder; central stabilizer.

1. Introduction

With the ever-growing span length of suspension bridges, one of the most challenging problems encountered is the aeroelastic stability at the design wind speed, ranging from 60 to 80 m/s. For the truss-girder suspension bridges, which have been mainly applied in the United States and Japan since the well known collapse of the original Tacoma Narrows Bridge in 1940, the design speed of 78 m/s was assumed for Akashi Kaikyo Bridge with the longest span length of 1991 m(Ueda, *et al*. 1988), while the value of 95 m/s (for one minute mean wind speed) or 80m/s (for ten minute speed) was defined for Tsing Ma Bridge with the second longest span length of 1377 m (Lau and Wong 1997). On the contrary, suspension bridges with streamline box decks have been prevailed in England, European Countries and China with lower design wind speed, for example, 60 m/s for Great Belt Bridge with the longest span of 1624 m (Larsen 1993) and 53 m/s for Runyang Bridge with the second longest span of 1490 m (Xiang, *et al*. 2003).

As a main section of the Zhoushan Island – Mainland Connection Project in Zhejiang Province, Xihoumen Bridge is proposed as a two span continuous suspension bridge with the centre span of 1650m, which is going to create a new record in box-deck suspension bridges. Based on the experience gained from Great Belt Bridge and Runyang Bridge mentioned above, the span length of 1500 m seems to be its intrinsic limit with box girders, even with the more strict stability

---

requirement of 80 m/s in Xihoumen Bridge (Ge, *et al*. 2003). In other words, the aerodynamic stability of this bridge should be guaranteed with some countermeasures, for example, cable system modifications, slotted deck solution, central stabilizers and passive and active control devices, whose performances have been reviewed elsewhere (Diana, *et al*. 1998, Xiang, *et al*. 2003).

Theoretical and experimental investigations reported in the literature (Matsumoto, *et al*. 1999, Matsumoto, *et al*. 2002, Tokoro, *et al*. 2001, Kimura, *et al*. 2005, Kubo, *et al*. 2005, Simiu and Miyata 2006) support the conclusion that the application of vertical stabilizers in the cross section center can improve aerodynamic stability of suspension bridges, for example, Akashi Kaikyo Bridge (Ueda, *et al*. 1988, Miyata 2002), Runyang Bridge (Xiang, *et al*. 2003), and an proposed super long suspension bridge with slotted box girder (Fumoto, *et al*. 2005). Further studies show that not only vertical stabilizers (central barriers) but also horizontal stabilizers (guide vanes) are effective to enhance critical flutter speed of suspension bridges (Ueda, *et al*. 1998). The investigation on aerodynamic and structural countermeasures for cable-stayed bridges with 2-edge I-shaped girder section indicated that the blocked central guard fence (a kind of central stabilizer) makes the flutter performance better in this kind of girder section (Murakami, *et al*. 2002). The central stabilizer was also proved to be effective on box girder section by wind tunnel tests (Fumoto, *et al*. 2005, Ge, *et al*. 2005, Murakami 2005). It was also found that the flutter performance of central-slotted box girder can be improved by center barrier (central stabilizer) and guide vane (horizontal stabilizer) (Sato, *et al*. 2000). Experimental evidence linking aerodynamic stability to stabilizer patterns and the ratio of the stabilizer height to the box depth are desirable for design purpose, but more detailed researches need to be done.

Taking as an example of Xihoumen Bridge, this paper presents the aerodynamic stabilization for long-span suspension bridges with box girders by using central stabilizers. The experimental investigation through sectional model testing was firstly carried out to obtain critical wind speeds corresponding to several stabilizer patterns and heights. The comprehensive evaluation of three central stabilizer patterns was then made through qualitative comparison and quantitative assessment, and an empirical expression based on Selberg formula was found for estimating critical wind speed of box-girder suspension bridges with central stabilizers. Finally, the stabilizing mechanism of central stabilizers for the box girder was revealed through comparison and contrast of aerodynamic derivatives, aerodynamic damping and degree participation levels among different heights of central stabilizer.

2. Experimental investigation with sectional model

In general, aerodynamic design of long-span suspension bridges such as the bridge scheme mentioned above will warrant elaborate experimental investigations including wind tunnel testing of alternative cross section designs and full aeroelastic bridge models for verification of final design. The objective of the experimental investigation described herein was to identify and assess effectiveness of central stabilizers for aerodynamic stabilization in suspension bridges with box girders. The wind tunnel testing with sectional models was adopted to this laborious and time-consuming aerodynamic investigations, leading to the selection of central stabilizers for box cross sections in the preliminary design (Ge, *et al*. 2003).

2.1. Objective model

The proposed Xihoumen Bridge is a two-span box girder suspension bridge with the span arrangement of 578 m + 1650 m + 485 m shown in Fig. 1. The streamlined box deck is 3.5 m deep

and 27.2 m in width allowing for four traffic lanes in the centre and one emergency parking lane on both sides shown in Fig. 2. With the emphasis on aerodynamic stability, the 1:80 sectional model for wind tunnel tests was designed to the objective model with the physical parameters including geometric dimensions, mass characteristics, fundamental frequencies and structural damping given in Table 1.

2.2. Stabilizer patterns

Following the way of vertical stabilizers, three stabilizer patterns were involved in the present study including a central stabilizer on the top of the box cross section called Stabilizer A, a
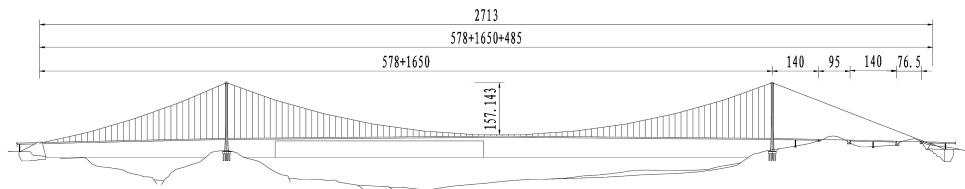
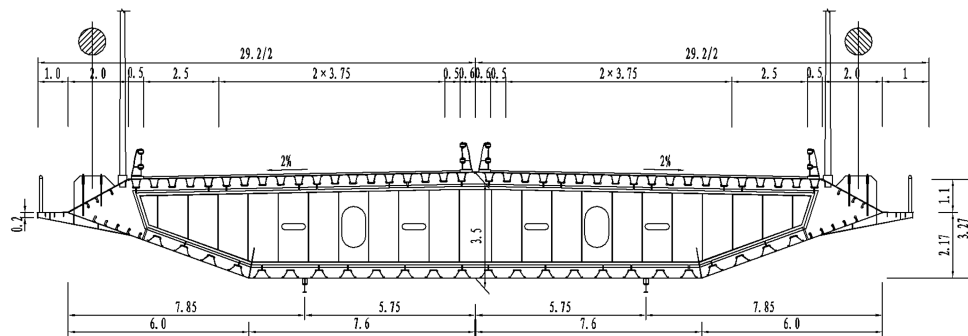Fig. 1 Elevation of Zhejiang Xihoumen Bridge (Unit: m)

Fig. 2 Original cross section (Unit: m)

Table 1 Physical parameters of objective model

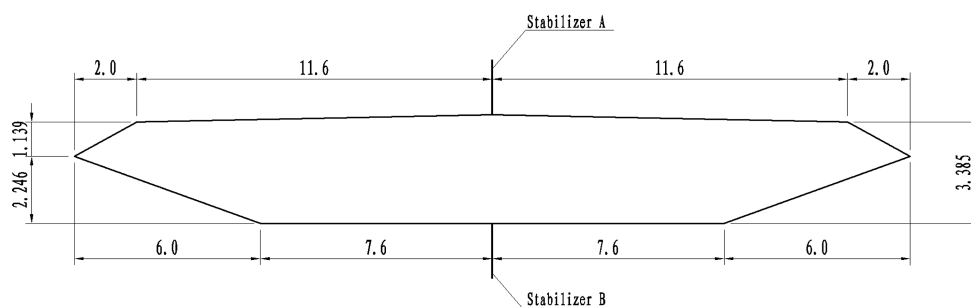| Parameter	Unit	Prototype	Scaling	Model
Length (L)	m		$\lambda_L = 1:80$	1.700
Width (B)	m	27.2	$\lambda_L = 1:80$	0.340
Depth (H)	m	3.385	$\lambda_L = 1:80$	0.042
Mass (m)	kg/m	28.2×10^3	$\lambda_m = 1:80^2$	4.406
Mass Moment (J_m)	kg-m^2/m	9.98×10^6	$\lambda_{Jm} = 1:80^4$	0.244
Bending Frequency (f_h)	Hz	0.1007	$\lambda_f = 80:6$	1.343
Torsional Frequency (f_t)	Hz	0.1995	$\lambda_f = 80:6$	2.660
Bending Damping (ξ_h)	%	0.5	$\lambda_\xi = 1:1$	0.5
Torsional Damping (ξ_h)	%	0.5	$\lambda_\xi = 1:1$	0.5
Required Speed (U)	m/s	80	$\lambda_V = 1:6$	13.3

Fig. 3 Simplified cross section (Unit: m)

stabilizer below the bottom namely Stabilizer B, and two stabilizers both on the top and below the bottom, Stabilizer A+B, shown in Fig. 3. In each pattern, the ratio of the stabilizer height h to the box depth H was respectively set to $h/H = 0$, 0.2, 0.4, 0.6 and 0.8.

2.3. Critical wind speeds

The wind tunnel testing of three central stabilizer patterns A, B and A+B was carried out in smooth flow at Tongji University's TJ-1 Boundary Layer Wind Tunnel with the working section of the 1.8 m width, the 1.8 m height and the 15m length. The wind tunnel tests were divided into two steps according to objectives. The objective of the first step was to detect the flutter critical speeds for the original cross section with Stabilizer A and deck attachments including light railings and guide edges described in Fig. 2, and then establish the influence of these deck attachments on the critical wind speed for the main purpose of the consulting workload (Ge, *et al*. 2003). The experimental results from the first step demonstrated that this influence can be approximately represented by a factor of 0.85, which is the ratio of the critical speed of the simplified section to that of the original section for cases with or without central stabilizers. On the contrary, the second step was purposely dedicated to further research and development including a more detailed investigation of stabilizer patterns and angle of attack on the critical wind speed, and measurements of eight aerodynamic derivatives of the simplified cross section for theoretical investigations of stabilizing mechanism.

The most important wind tunnel test result links the critical wind speed of the box cross section to the height of central stabilizer for the cases at the attack angles of +3°, 0° and -3°, and is summarized in Table 2. Measured critical wind speeds are made in full scale by multiplication with the wind speed factor of $\lambda_v = 6$.

Table 2 Experimental results of critical wind speed (m/s)

h/H	Stabilizer A			Stabilizer B			Stabilizer A+B		
	+3°	0°	-3°	+3°	0°	-3°	+3°	0°	-3°
0	87.0	90.0	98.4	87.0	90.0	98.4	87.0	90.0	96.4
0.2	91.2	115.2	109.8	90.0	110.4	111.6	72.0	108.6	127.2
0.4	96.0	118.8	102.0	82.8	102.0	112.8	106.2	102.0	87.0
0.6	111.0	105.0	96.0	72.0	99.0	110.4	108.6	91.8	
0.8	121.2	94.8	91.2	55.8	91.2	95.4			

3. Comprehensive evaluation of central stabilizers

It can be seen from Table 2 that the stabilizing effectiveness of central stabilizer generally depends upon three important characteristics, including stabilizer patterns, height of stabilizer and angle of attack. Since critical wind speeds change with these three characteristics following very sophisticated relationships, the comprehensive evaluation of central stabilizers was conducted in the sequence starting from qualitative comparison of three stabilizer patterns to determine effective ones, followed by quantitative assessment of effective patterns determined, and finally to empirical regression of critical wind speeds experimentally identified and theoretically calculated by Selberg formula.

3.1. Qualitative comparison

Table 2 demonstrates a clear fact that the values of critical wind speeds vary with angle of attack for all cases with or without central stabilizers having various heights. Since aerodynamic instability takes place whenever a bridge is exposed to wind speeds above the critical value at the attack angles covering from +3º to -3º according to Chinese code, the dominant factor of aerodynamic stability is the minimum value among three critical wind speeds corresponding to the +3º, 0º and -3º angle of attack for the certain stabilizer pattern with the certain height of stabilizer. The minimum critical wind speeds, therefore, are extracted for three certain stabilizer patterns with five heights of stabilizer and described in Fig. 4.

Based on the minimum values of critical wind speed shown in Fig. 4, both Stabilizers A and B can improve aerodynamic stability at the certain height of stabilizers for suspension bridges with box girders. In particular, the critical wind speed increases with the relative stabilizer height from $h/H = 0$ to $h/H = 0.6$ for Stabilizer A and from $h/H = 0$ to $h/H = 0.2$ for Stabilizer B, respectively, but decreases with the relative height from $h/H = 0.6$ to $h/H = 0.8$ for Stabilizer A and from $h/H = 0.2$ to $h/H = 0.8$ for Stabilizer B, respectively. Stabilizer A+B, however, makes it impossible to increase critical wind speed at any relative height of stabilizer, and is thus not discussed below.
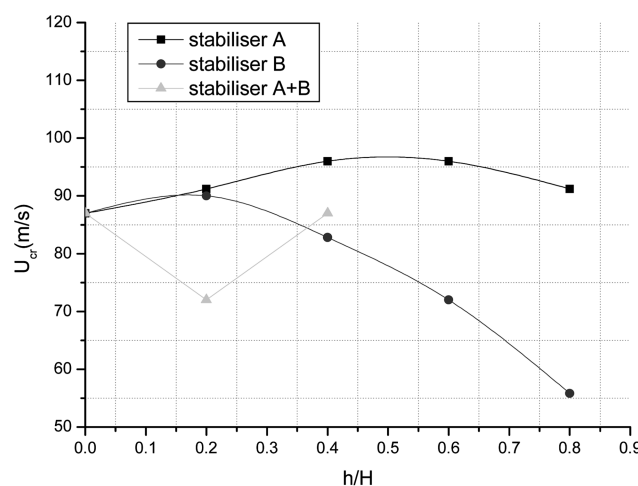

Fig. 4 Minimum values of critical wind speed

3.2. Quantitative assessment

In order to quantitatively evaluate stabilizing effect of Stabilizers A and B, the relative factor of critical wind speed is defined as follows:

$$\eta = \frac{U_{crh}}{U_{cro}} \tag{1}$$

where U_{cro} is the critical wind speed of the box section without central stabilizer; and U_{crh} is the critical wind speed with the stabilizer of h. The relations between relative factor η and relative stabilizer height h/H are represented in Fig. 5 for both Stabilizers A and B. In the case of Stabilizer A, the value of the relative factor η is always greater than unit for all relative stabilizer heights h/H, from 0 to 0.8, and reach the maximum of 1.113 at $h/H = 0.5$ following the fitted curve of the measured critical wind speeds. The relative factor η of Stabilizer B has the value greater than unit only from $h/H = 0$ to $h/H = 0.3$, and the maximum value of 1.041 at $h/H = 0.137$ by the fitted data of the critical wind speeds. Since the maximum relative factor is very small and effective height is quite narrow, Stabilizer B is quantitatively assessed as an unfavorable stabilizer pattern for application in aerodynamic stabilization of suspension bridges with box girders.

3.3. Empirical expression

With considering the application of Stabilizer A in the proposed bridge project, a Lorentz peak-value function was fitted to the measured critical wind speeds by means of the least squares method. The following empirical expression was obtained for calculating the critical wind speed of box girders with Stabilizer A.

$$\frac{U_{cr}^{Sta}}{U_{cr}^{Sel}} = \eta_{h/H} = 0.92 + \frac{0.136}{0.7 + 4(0.5 - h/H)^2} \tag{2}$$

where U_{cr}^{Sel} is critical wind speed defined by Selberg formula (Selberg 1963). Fig. 5 depicts the
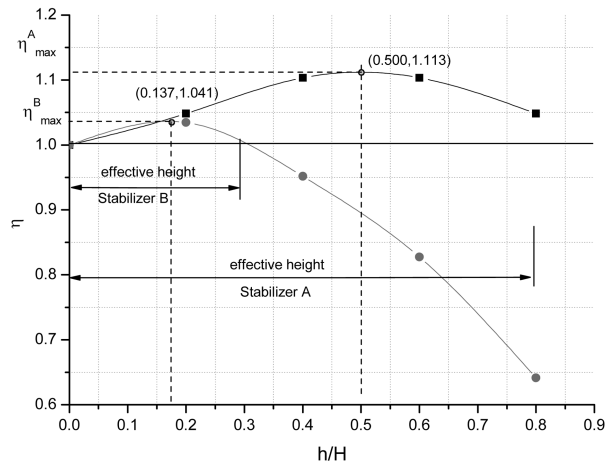

Fig. 5 Relative factor of critical wind speed

diagram of the relative factor of critical wind speed versus the relative height h/H of Stabilizer A.

The critical wind speed U_{cr}^{Sta} of box girders with Stabilizer A may now be predicted from a modified Selberg formula as follow:

$$U_{cr}^{Sta} = \eta_{h/H}\kappa f_t \sqrt{\frac{\sqrt{mJ_m}}{\rho B}\left[1-\left(\frac{f_h}{f_t}\right)^2\right]} \tag{3}$$

where m is mass of sectional model in the unit of kg/m; J_m is mass moment of inertia of sectional model in kg-m^2/m; ρ is air density in kg/m^3; B is width of sectional model in m; f_h is the fundamental frequency in vertical bending in Hz; f_t is the fundamental frequency in torsion in Hz; and κ is shape factor of sectional model with $\kappa = 4.0$.

4. Theoretical analysis of stabilizing mechanism

Analytical and experimental studies in bridge aerodynamics began immediately following the fall of Tacoma Narrows in 1940, but the generation mechanism of flutter instability had not been well uncovered until very recent. Based on the concept of full-degree coupling analysis, a two-dimensional three-degree-of-freedom flutter analysis method, which can simultaneously investigate the relationship between oscillation parameter of three degrees of freedom and aerodynamic derivatives obtained by wind tunnel testing with sectional model tests, and can clarify the coupling effect of each DOF in flutter instability, was proposed by the authors to reveal the driven mechanism of flutter oscillation (Yang 2002, Yang, *et al.* 2002, 2003), and was thus applied in the theoretical analysis of stabilizing mechanism of this cross section with the references of flutter derivatives, aerodynamic damping and degree participation.

4.1. Flutter derivatives

For a two-dimensional section model with three degrees of freedom including heaving, swaying and torsion, the equation of motion can be expressed by eighteen flutter derivatives as follows (Yang 2002):

$$J_m(\ddot{\alpha}+2\xi_{\alpha s}\omega_{\alpha s}\dot{\alpha}+\omega_{\alpha s}^2\alpha)=\frac{1}{2}\rho U^2(2B^2)\left[KA_1^*\frac{\dot{h}}{U}+KA_2^*\frac{B\dot{\alpha}}{U}+K^2A_3^*\alpha+K^2A_4^*\frac{h}{B}+KA_5^*\frac{\dot{p}}{U}+K^2A_6^*\frac{p}{B}\right] \tag{4}$$

$$m_h(\ddot{h}+2\xi_{hs}\omega_{hs}\dot{h}+\omega_{hs}^2h)=\frac{1}{2}\rho U^2(2B)\left[KH_1^*\frac{\dot{h}}{U}+KH_2^*\frac{B\dot{\alpha}}{U}+K^2H_3^*\alpha+K^2H_4^*\frac{h}{B}+KH_5^*\frac{\dot{p}}{U}+K^2H_6^*\frac{p}{B}\right] \tag{5}$$

$$m_p(\ddot{p}+2\xi_{ps}\omega_{ps}\dot{p}+\omega_{ps}^2p)=\frac{1}{2}\rho U^2(2B)\left[KP_1^*\frac{\dot{h}}{U}+KP_2^*\frac{B\dot{\alpha}}{U}+K^2P_3^*\alpha+K^2P_4^*\frac{h}{B}+KP_5^*\frac{\dot{p}}{U}+K^2P_6^*\frac{p}{B}\right] \tag{6}$$

where m_h, m_p and J_m are mass and mass moment of inertia in the corresponding degrees of freedom; ξ_{hs}, ξ_{ps} and $\xi_{\alpha s}$ are structural damping ratios of the corresponding degrees of freedom; ω_{hs}, ω_{ps} and $\omega_{\alpha s}$ are natural circular frequencies of the corresponding degrees of freedom; ρ is air mass density; B is bridge deck width; U is wind velocity; K is reduced frequency with $K = B\omega/U$; and ω is the circular frequency of response; and H_i^*, P_i^* and A_i^* ($i = 1, 2, \ldots, 6$) are dimensionless flutter

derivatives measured in wind tunnel tests.

These eighteen flutter derivatives can be broadly divided into two groups, aerodynamic stiffness related derivatives and aerodynamic damping related derivatives. In general, the latter plays more important role in stabilizing mechanism. With the simplification of two degrees of freedom including heaving and torsion, four damping related derivatives, A_1^*, A_2^*, H_1^* and H_2^* are shown in Fig. 6 for Stabilizer A with the relative heights of $h/H = 0$, $h/H = 0.2$ and $h/H = 0.8$ at the $+3^\circ$ angle of attack. Since the critical wind speed increases with the increase of the relative height from $h/H = 0$ to $h/H = 0.8$ at $+3^\circ$ described in Table 2, it can be concluded from Fig. 6 that there is no clear trend for the cross section with Stabilizer A to become increasingly aerodynamically stable for increasing the absolute magnitude of damping related derivatives.

4.2. Aerodynamic damping

With the equations of motion expressed by Eqs. (4), (5) and (6), oscillation frequencies and damping ratios of three degrees of a two-dimensional section model can be derived and represented by the combination of flutter derivatives and phase lags between motions having the same oscillation frequency. Through double iterations of wind speed and oscillation frequency, the total damping ratios can be written by the following formulas (Yang 2002).
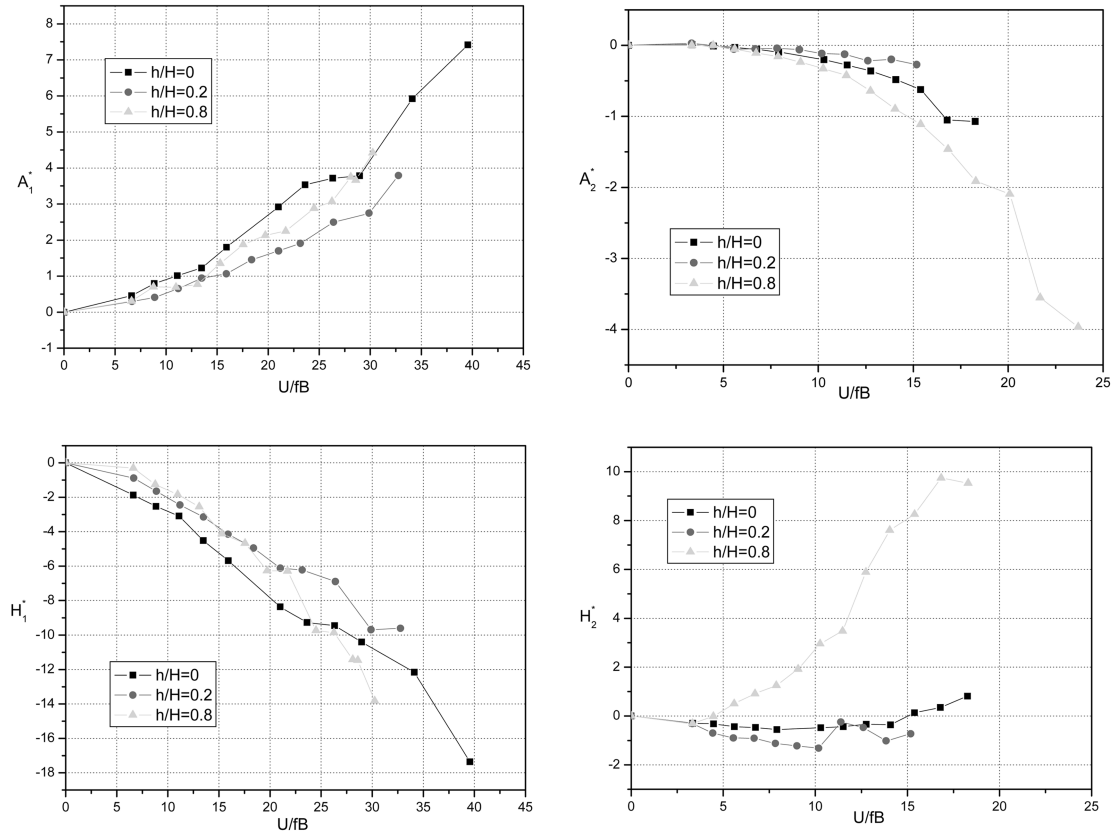

Fig. 6 Aerodynamic damping related derivatives

$$\xi_\alpha = \frac{\xi_{as}\omega_{as}}{\omega_\alpha} - \frac{1}{2}\frac{\rho B^4}{I}A_2^*$$

$$-\frac{1}{2}\frac{\rho B^4}{I}\frac{\rho B^2}{m_h}\Omega_{h\alpha}\left[A_1^*H_3^*\cos\theta_{\alpha h} - A_4^*H_3^*\sin\theta_{\alpha h} + A_1^*H_2^*\cos\left(\theta_{\alpha h} + \frac{3}{2}\pi\right) - A_4^*H_2^*\sin\left(\theta_{\alpha h} + \frac{3}{2}\pi\right)\right] \qquad (7)$$

$$-\frac{1}{2}\frac{\rho B^4}{I}\frac{\rho B^2}{m_p}\Omega_{p\alpha}\left[A_5^*P_3^*\cos\theta_{\alpha p} - A_6^*P_3^*\sin\theta_{\alpha p} + A_5^*P_2^*\cos\left(\theta_{\alpha p} + \frac{3}{2}\pi\right) - A_6^*P_2^*\sin\left(\theta_{\alpha p} + \frac{3}{2}\pi\right)\right]$$

$$\xi_h = \frac{\xi_{hs}\omega_{hs}}{\omega_h} - \frac{1}{2}\frac{\rho B^2}{m_h}H_1^*$$

$$-\frac{1}{2}\frac{\rho B^4}{I}\frac{\rho B^2}{m_h}\Omega_{\alpha h}\left[H_2^*A_4^*\cos\theta_{h\alpha} - H_3^*A_4^*\sin\theta_{h\alpha} + H_2^*A_1^*\cos\left(\theta_{h\alpha} + \frac{3}{2}\pi\right) - H_3^*A_1^*\sin\left(\theta_{h\alpha} + \frac{3}{2}\pi\right)\right] \qquad (8)$$

$$-\frac{1}{2}\frac{\rho B^2}{m_h}\frac{\rho B^2}{m_p}\Omega_{ph}\left[H_5^*P_4^*\cos\theta_{hp} - H_6^*P_4^*\sin\theta_{hp} + H_5^*P_1^*\cos\left(\theta_{hp} + \frac{3}{2}\pi\right) - H_6^*P_1^*\sin\left(\theta_{hp} + \frac{3}{2}\pi\right)\right]$$

$$\xi_p = \frac{\xi_{ps}\omega_{ps}}{\omega_p} - \frac{1}{2}\frac{\rho B^2}{m_p}P_5^*$$

$$-\frac{1}{2}\frac{\rho B^4}{I}\frac{\rho B^2}{m_p}\Omega_{\alpha p}\left[P_2^*A_6^*\cos\theta_{p\alpha} - P_3^*A_6^*\sin\theta_{p\alpha} + P_2^*A_5^*\cos\left(\theta_{p\alpha} + \frac{3}{2}\pi\right) - P_3^*A_5^*\sin\left(\theta_{p\alpha} + \frac{3}{2}\pi\right)\right] \qquad (9)$$

$$-\frac{1}{2}\frac{\rho B^2}{m_h}\frac{\rho B^2}{m_p}\Omega_{hp}\left[P_1^*H_6^*\cos\theta_{ph} - P_4^*H_6^*\sin\theta_{ph} + P_1^*H_5^*\cos\left(\theta_{ph} + \frac{3}{2}\pi\right) - P_4^*H_5^*\sin\left(\theta_{ph} + \frac{3}{2}\pi\right)\right]$$

where ω_h, ω_p and ω_α are iterative circular frequencies of the corresponding degrees of freedom; Ω_{ij} is dimensionless equivalent frequency between two motions and is defined as

$$\Omega_{ij} = \frac{\omega_i^2}{\sqrt{(\omega_j^2 - \omega_i^2)^2 + 4(\xi_i\omega_i\omega_j)^2}} \quad (i, j = \alpha, h, p) \qquad (10)$$

and θ_{ij} is phase lag between two motions and is expressed as

$$\theta_{ij} = arctg\frac{2\xi_j\omega_j\omega_i}{\omega_j^2 - \omega_i^2} \quad (i, j = \alpha, h, p) \qquad (11)$$

In the case of either two-degree-of-freedom coupled flutter or one-degree-of-freedom torsional flutter, the most important aerodynamic damping is in torsional vibration. With considering two-degree-of-freedom vibration, aerodynamic damping ratio in torsion can be represented by the summation of five parts as follows.

$$A = -\frac{1}{2}\frac{\rho B^4}{J_m}A_2^* \qquad (12)$$

$$B = -\frac{1}{2}\frac{\rho B^4}{J_m}\frac{\rho B^2}{m_h}\Omega_{\alpha h}A_1^* H_3^* \cos\theta_{\alpha h} \tag{13}$$

$$C = \frac{1}{2}\frac{\rho B^4}{J_m}\frac{\rho B^2}{m_h}\Omega_{\alpha h}A_4^* H_3^* \sin\theta_{\alpha h} \tag{14}$$

$$D = -\frac{1}{2}\frac{\rho B^4}{J_m}\frac{\rho B^2}{m_h}\Omega_{\alpha h}A_1^* H_2^* \cos\left(\theta_{\alpha h}+\frac{3}{2}\pi\right) \tag{15}$$

$$E = \frac{1}{2}\frac{\rho B^4}{J_m}\frac{\rho B^2}{m_h}\Omega_{\alpha h}A_4^* H_2^* \sin\left(\theta_{\alpha h}+\frac{3}{2}\pi\right) \tag{16}$$

Fig. 7 describes the evolution of these five parts for Stabilizer A with $h/H = 0$, $h/H = 0.2$ and $h/H = 0.8$ at the $+3^\circ$ angle of attack. Part A with the reference of A_2^* is always positive and makes the greatest contribution to aerodynamic stability among five parts for all three cases, while Part B with the reference of $A_1^* H_3^*$ keeps negative all the way and causes the worst influence of aerodynamic stability. Both Parts C and D can help in stability at $h/H = 0$ and $h/H = 0.2$ or not at $h/H = 0.8$ with smaller value, and the influence of Part E is helpful to stability but with the smallest effect. It should be noted that aerodynamic damping ratio in torsion is decided by not only single damping related derivative, A_2^*, but also derivative couples, $A_1^* H_3^*$, $A_1^* H_2^*$, $A_4^* H_3^*$ and $A_4^* H_2^*$. The total damping ratios including structural one and these five parts are shown in Fig. 8 for these three cases, as well as $h/H = 0.8$ at the attack angles of 0° and -3°.

4.3. Degree participation

Based on the above full-degree coupling formulations, the two-dimensional three-degree-of-freedom flutter analysis can be performed to simultaneously investigate the relationship between systematic oscillation parameters and aerodynamic derivatives, and one of the most important result of this analysis is the coupling effect of degrees of freedom in flutter oscillation. The participation level of motion in each degree of freedom at the flutter onset can be described by three flutter modality vectors with the endpoints as follows (Yang 2002).
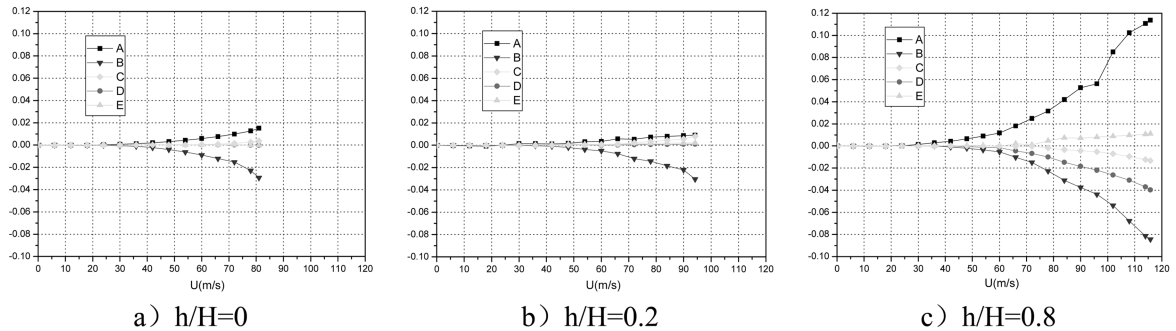

a）h/H=0   b）h/H=0.2   c）h/H=0.8

Fig. 7 Aerodynamic damping ratios
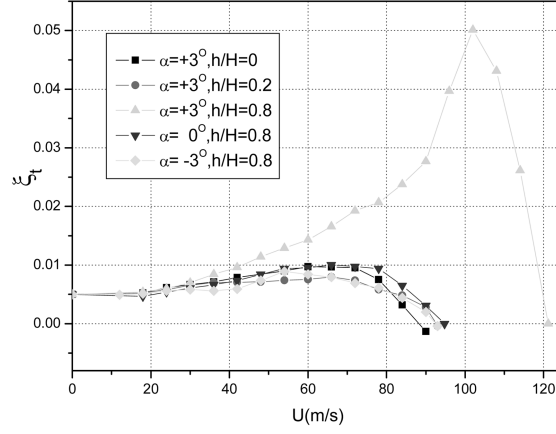
Fig. 8 Total damping ratios

$$V_\alpha = \left(\frac{1}{C_\alpha}, \frac{\rho B^2 \Omega_{h\alpha} \sqrt{H_2^{*2} + H_3^{*2}}}{m_h C_\alpha}, \frac{\rho B^2 \Omega_{p\alpha} \sqrt{P_2^{*2} + P_3^{*2}}}{m_p C_\alpha} \right) \tag{17}$$

$$V_h = \left(\frac{\rho B^4 \Omega_{\alpha h} \sqrt{A_1^{*2} + A_4^{*2}}}{J_m C_h}, \frac{1}{C_h}, \frac{\rho B^2 \Omega_{ph} \sqrt{P_1^{*2} + P_4^{*2}}}{m_p C_h} \right) \tag{18}$$

$$V_p = \left(\frac{\rho B^4 \Omega_{\alpha p} \sqrt{A_5^{*2} + A_6^{*2}}}{J_m C_p}, \frac{\rho B^2 \Omega_{hp} \sqrt{H_5^{*2} + H_6^{*2}}}{m_h C_p}, \frac{1}{C_p} \right) \tag{19}$$

where

$$C_\alpha = \sqrt{1 + \left(\frac{\rho B^2}{m_h} \Omega_{\alpha h} \sqrt{H_2^{*2} + H_3^{*2}} \right)^2 + \left(\frac{\rho B^2}{m_p} \Omega_{\alpha p} \sqrt{P_2^{*2} + P_3^{*2}} \right)^2} \tag{20}$$

$$C_h = \sqrt{\left(\frac{\rho B^4}{J_m} \Omega_{h\alpha} \sqrt{A_1^{*2} + A_4^{*2}} \right)^2 + 1 + \left(\frac{\rho B^2}{m_p} \Omega_{hp} \sqrt{P_1^{*2} + P_4^{*2}} \right)^2} \tag{21}$$

$$C_p = \sqrt{\left(\frac{\rho B^4}{J_m} \Omega_{p\alpha} \sqrt{A_5^{*2} + A_6^{*2}} \right)^2 + \left(\frac{\rho B^2}{m_h} \Omega_{ph} \sqrt{H_5^{*2} + H_6^{*2}} \right)^2 + 1} \tag{22}$$

For the above-mentioned five cases in two-degree vibration, the degree participation and the corresponding critical wind speed at the flutter onset can be represented in Fig. 9 and Table 3. The box section with Stabilizer A of $h/H = 0.8$ at the $+3°$ angle of attack has the highest level of heaving degree participation and the greatest critical wind speed, while the box section without stabilizer has the lowest values of both coupling effect of heaving degree and critical wind speed. In general, it can be concluded that the more heaving degree participate at the flutter onset, the higher critical wind speed can be reached.
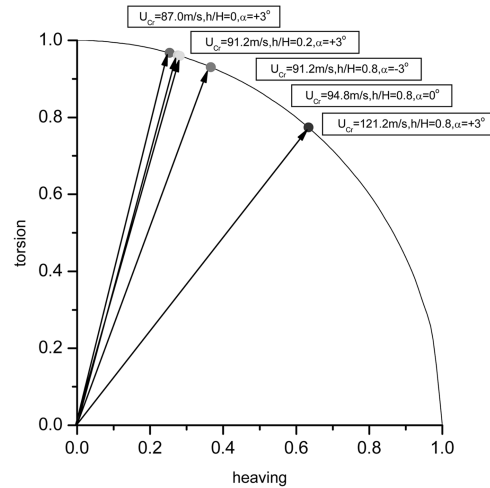
Fig. 9 Degree participation level

Table 3 Torsional and heaving degrees particiaption in flutter mode

Degree Participation	h/H = 0 $\alpha = +3°$	h/H = 0.2 $\alpha = +3°$	h/H = 0.8 $\alpha = -3°$	h/H = 0.8 $\alpha = 0°$	h/H = 0.8 $\alpha = +3°$
V_α	0.967	0.961	0.959	0.931	0.774
V_h	0.254	0.276	0.282	0.366	0.634
U_{cr} (m/s)	87.0	91.2	91.2	94.8	121.2

5. Conclusions

Based on the recent project of Xihoumen Bridge in China, aerodynamic stabilization of central stabilizers was carefully investigated for long-span suspension bridges with box girders through experimental investigation, comprehensive evaluation and theoretical analysis. Wind tunnel tests with sectional models, which were designed as the simplified cross sections due to Xihoumen Bridge, were firstly conducted to detect critical wind speeds for three patterns of central stabilizers. With the experimental results of wind tunnel tests, Stabilizer A was then concluded as the best pattern to stabilize box girders aerodynamically, after having made comparison and contrast qualitatively and quantitatively among Stabilizer A, B and A+B, and a modified Selberg formula was accordingly fitted for estimating critical wind speed of box-girder suspension bridges using Stabilizer A. Based on the concept of full-degree coupling analysis, theoretical investigation of stabilization mechanism was finally carried out with the references of flutter derivatives, aerodynamic damping and degree participation. It can be concluded that aerodynamic damping is the most important factor in stabilization consists of five varying parts represented by flutter derivatives, whose absolute values have no clear relation with aerodynamic stability, and the more heaving degree involves in two-degree-of-freedom coupled flutter, the higher critical wind speed can be guaranteed.

Acknowledgements

References

Diana, G., Bruni, S., Collina, A. and Zasso, A. (1998), "Aerodynamic Challenges in Super Long Span Bridge Design", *Bridge Aerodynamics*, Larsen & Esdahl (eds), Balkema, Rotterdam, 131-143.

Fumoto, K., Hata, K., Kusuhara, S., Shirai, S., Hatanaka, A. and Yamaguchi, E. (2005), "Aerodynamic Stabilization of Flat Box Girder in Super Long-Span Suspension Bridge", *Proc. of the 6th Asia-Pacific Conf. on Wind Engineering*, Seoul, Korea, 1249-1264.

Fumoto, K., Hata, K., Matsuda, K., Murakami, T., Saito, Y. and Shirai, S. (2005), "Aerodynamic Improvement of Slotted One-Box Girder Section for Super Long Suspension Bridge", *Proc. of the 6th Asia-Pacific Conf. on Wind Engineering*, Seoul, Korea, 1222-1236.

Fumoto, K., Kusuhara, S., Oryu, T., Suzawa, M., Yoshizumi, F. and Hirai, S. (2005), "Large-Scale Wind Tunnel Test of Super Long Suspension Bridge with Slotted One-Box Girder", *Proc. of the 6th Asia-Pacific Conf. on Wind Engineering*, Seoul, Korea, 1211-1221.

Ge, Y.J., *et al.* (2003), *Study of Aerodynamic Performance and Vibration Control of Xihoumen Bridge* (in Chinese), Technical Report of the State Key Laboratory for Disaster Reduction in Civil Engineering, No. WT200320.

Ge, Y.J., Zou, X.J. and Yang, Y.X. (2005), "Aerodynamic Stabilization of Long-Span Suspension Bridges with Box Girders Using Central Stabilizers", *Proc. of the 6th Asia-Pacific Conf. on Wind Engineering*, Seoul, Korea, 1237-1248.

Kimura, K., Tanaka, Y., Utsunomiya, M., Kubo, Y. (2005), "An Analytical Study on Flutter Improvement by Combining Stiffening Girders with Different Cross-Sectional Shapes", *Proc. of the 6th Asia-Pacific Conf. on Wind Engineering*, Seoul, Korea, 839-851.

Kubo, Y., Tsuji, E., Yoshida, K., Kimura, K. and Kato, K. (2005), "Development of bridge deck section for a super long bridge by applying the Separation Interference Method", *Proc. of the 6th Asia-Pacific Conf. on Wind Engineering*, Seoul, Korea, 2065-2074.

Larsen, A. (1993), "Aerodynamic Aspects of the Final Design of the 1624m Suspension Bridge across the Great Belt", *J. Wind Eng. Ind. Aerod.*, **48**, 261-285.

Lau, C.K. and Wong, K.Y. (1997), "Aerodynamic Stability of Tsing Ma Bridge", *Structures in the New Millennium*, Lee (ed.), Balkema, Rotterdam, 131-138.

Matsumoto, M., Yoshzumi, F., Yabutani, T., Abe, K. and Nakajima, N. (1999), "Flutter Stabilization and Heaving-Branch Flutter", *J. Wind Eng. Ind. Aerod.*, **83**.

Matsumoto, M., Shirato, H., Shijo, R., *et al.* (2002), "Flutter Stabilization of Long Span Bridges", *Proc. of the 2nd Int. Symposium on Advances in Wind and Structures*, Busan, Korea, 257-264.

Miyata, T. (2002), "Significance of aero-elastic relationship in wind-resistant design of long-span bridges", *J. Wind Eng. Ind. Aerod.*, **90**, 1479-1492.

Murakami, T., Takeda, K., Takao, M. and Yui, R. (2002), "Investigation on aerodynamic and structural countermeasures for cable-stayed bridge with 2-edge I-shaped girder", *J. Wind Eng. Ind. Aerod.*, **90**, 2143-2151.

Murakami, T. (2005), "Effects of Angle of Attack on Flutter Instability of Mono-Box Girder Section with Center Barrier", *Proc. of the 6th Asia-Pacific Conf. on Wind Engineering*, Seoul, Korea, 1265-1273.

Sato, H., Kusuhara, S., Ogi, K.I. and Matsufuji, H. (2000), "Aerodynamic characteristics of super long-span bridges with slotted box girder", *J. Wind Eng. Ind. Aerod.*, **88**, 297-306.

Selberg, A. (1963), "Aerodynamic Effect on Suspension Bridges", *Proc. of Int. Symposium on Wind Effects on Buildings and Structures*, Teddington, England, **2**, 462-486.

Simiu, E. and Miyata, T. (2006), *Design of Buildings and Bridges for Wind: A Practical Guide for ASCE 7 Users and Designers of Special Structures*, John Wiley and Sons, New York.

Tokoro, S., Honda, A., Masuda, I. and Nakashima, Y. (2001), "Flutter Stability of Super-Long Suspension Bridges Employing Wind Shields", *J. Wind Eng.*, No. 89, 477-480 (in Japanese).

Ueda, T., Yasuda, M. and Nakagaki, R. (1988), "Mechanism of Aerodynamic Stabilization for Long-span

Suspension Bridge with Stiffening Truss-Girder", *J. Wind Eng.*, No.37, 477-484 (in Japanese).

Ueda, T., Tanaka, T. and Matsushita, Y. (1998), "Aerodynamic Stabilization for Super Long-Span Suspension Bridges", *Proc. of IABSE Symposium - Long Span and High Rise Structures*, Kobe, Japan, 721-728.

Xiang, H.F., *et al.* (2003), *Wind Resistance Study on Runyang Suspension Bridge across Yangtze River*, Technical Report of the State Key Laboratory for Disaster Reduction in Civil Engineering, No. WT200005.

Xiang, H.F. and Ge, Y.J. (2003), "On Aerodynamic Limit to Suspension Bridges", *Proc. of the 11th Int. Conf. on Wind Engineering*, Texas, USA, 65-80.

Yang, Y.X. (2002), "Two-Dimensional Flutter Mechanism and its Applications for Long-Span Bridges", Ph.D Thesis Supervised by H.F. Xiang, and Y.J. Ge, Tongji University, China (in Chinese).

Yang, Y.X., Ge, Y.J. and Xiang, H.F. (2002), "Coupling Effects of Degrees of Freedom in Flutter Instability of Long-Span Bridges", *Proc. of the 2nd Int. Symposium on Advances in Wind and Structures*, Busan, Korea, 625-632.

Yang, Y.X., Ge, Y.J. and Xiang, H.F. (2003), "3DOF Coupling Flutter Analysis for Long-Span Bridges", *Proc. of the 11th Int. Conf. on Wind Engineering*, Texas, USA, 925-932.

CC